Pergamon

Int. J. Heat Mass Transfer. Vol. 41, No. 10, pp. 1149–1156, 1998

Printed in Great Britain
0017–9310/98 $19.00+0.00

PII: S0017–9310(97)00251–2

Unsteady heat transfer and velocity of a cylinder in cross flow—II. High freestream turbulence

J. W. SCHOLTEN and D. B. MURRAY

Department of Mechanical Engineering, Trinity College, Dublin 2, Ireland

(*Received* 22 *January* 1997 *and in final form* 21 *August* 1997)

Abstract—This paper is the second of two papers which describe the simultaneous measurement of time resolved heat flux and local velocity at the surface of a cylinder in cross flow. Tests are conducted with high freestream turbulence for a range of Reynolds numbers and transition to turbulence occurs within the boundary layer on the cylinder. The coherence and phase difference between the velocity and heat flux signals are used to deduce that, in contrast to the low freestream turbulence case considered in Part I, most of the heat transfer fluctuations at the front of the cylinder originate in the small turbulent eddies present in the flow. © 1998 Elsevier Science Ltd.

INTRODUCTION

In many engineering situations in which a cylinder is used as a heat transfer surface, the mainstream flow around the cylinder contains a high level of velocity fluctuations. This increased level of turbulence may already exist in the flow, as in an unconditioned duct flow, or is a consequence of upstream cylinders, as in the case of tubular heat exchangers.

The influence of freestream turbulence on the time-average Nusselt numbers of cylinders in cross flow has formed the subject of numerous experimental investigations. For example, the combined effect of freestream turbulence and tunnel blockage on average Nusselt numbers was reviewed by Morgan [1] and the influence of turbulence intensity on local heat transfer levels was investigated by Dyban and Epick [2] and Lowery and Vachon [3]. However, for the identification of convective heat transfer mechanisms, measurements of unsteady heat transfer are more useful. This is particularly the case for applications involving high turbulence levels as significant fluctuations in local fluid velocity are likely to produce corresponding fluctuations in surface heat flux. Simultaneous measurement of the fluctuating heat flux and velocity signals could lead to an improved understanding of the link between local flow structure and surface heat transfer. For a cylinder in a cross flow of high turbulence intensity, Simmons *et al.* [4] and Ching and O'Brien [5] have reported fluctuations in the heat transfer from measurements in the stagnation region of a cylinder. However, no measurements were reported for other locations on the tube circumference.

This paper describes a study in which simultaneous measurements of time-resolved heat flux and local fluid velocity are obtained at the surface of a cylinder in cross flow with a high freestream turbulence. Tests are conducted for a range of Reynolds numbers and, because of the elevated freestream turbulence, transition to turbulence is seen to occur within the boundary layer on the cylinder. The heat transfer results are reported in the form of auto spectra and time traces, together with the variation in time averaged Nusselt numbers around the circumference. From the simultaneous measurements, the coherence and phase difference between the velocity and heat flux signals are examined, with a view to identifying the origin of the surface heat transfer fluctuations. The results are compared with those obtained in Part I for low freestream turbulence levels and some fundamental aspects of the interaction between convective heat transfer and the turbulence structure for cylinders in cross flow are explored.

EXPERIMENTAL SET-UP AND DATA PROCESSING

The measurements were carried out using the wind tunnel, test cylinder and system of instrumentation described in Part I. Briefly, the test cylinder consists of a 25 mm diameter, internally heated copper tube with a surface mounted Dantec 55R47 hot film sensor. The hot film was connected to a Dantec 55M10 standard wheatstone bridge which kept the film temperature constant with a 0.5°C overheat with respect to the temperature of the tube surface. The frequency response of the sensor was estimated as approximately 10 kHz. The heat transfer rates were calculated by dividing the electrical power dissipated in the hot film by the effective surface area of the hot film, Beasley and Figliola [6].

The velocity measurements were obtained with a laser Doppler system which consisted of a 32 mW HeNe laser with Bragg cell for frequency shifting. It was used in the forward scatter mode and the pho-

NOMENCLATURE

Nu	Nusselt number	Re	Reynolds number
Nu_{fsp}	Nusselt number at front stagnation point	Tu	turbulence intensity [%]
Nu'	Nusselt number fluctuations	U	upstream velocity [m/s].

tomultiplier signal was processed by a TSI 1980B counter type processor. Simultaneous velocity and heat flux measurements were recorded through the direct memory access (DMA) technique into the computer, with a triggering pulse from the LDA-counter processor being used to start AtoD conversions. The data were resampled at equidistant time intervals by using a 1st order interpolation, Simon *et al.* [7].

In order to assess the influence of mainstream turbulence on the fluctuations in surface heat flux, a turbulence grid was installed 55 mm upstream of the instrumented cylinder. The main stream turbulence intensities thus obtained are in the range 6.7–8.5%, with the variation in turbulence levels as a function of velocity being given in Table 1. This contrasts with turbulence levels of 0.3–1.3% for the tests conducted without the grid, as described in Part I.

RESULTS

As in Part I, the results are presented in the form of plots of time-averaged Nusselt numbers together with the root mean square (rms) of the Nusselt number fluctuations as a function of the angular location. In addition, the results are presented in the form of heat transfer auto spectra and time traces. From the simultaneous sampling measurements, results for the coherence and phase have been included. In order to facilitate comparison, the range of velocities and Reynolds numbers for which measurements were obtained is very similar to that used in the low turbulence tests described in Part I.

Time-averaged data and variation in local Nusselt number

Figures 1–3 show the time-averaged local Nusselt number, and the rms of the local Nusselt number fluctuations, for the turbulent freestream flow with Reynolds numbers from 7190 to 43 140. The Reynolds number of 50 350, used in the low turbulence tests described in Part I, could not be reached due to the increased flow resistance caused by the turbulence grid. The Nusselt numbers have been corrected for the insulating effect of the sensor substrate, Scholten and Murray [8]. It can be seen from the rms plots that, for all the Reynolds numbers used, the level of fluctuations over the front of the cylinder is almost as high as in the wake. This contrasts with the extremely low rms values over the cylinder front reported in Part I for the equivalent low turbulence tests. Furthermore, it can be seen that the shape of the average Nusselt number plot changes in character with an increase in the Reynolds number. This change in shape is consistent with transition to turbulence within the boundary layer. For the present conditions, the transition Reynolds number is around 21 000. This can be seen from Fig. 2(a), in which the change in character for some locations has occurred, leading to abrupt local changes in the time-averaged Nusselt number. The characteristic of abrupt variations in Nusselt number at around 100° is repeatable although the local heat transfer pattern may not be replicated exactly.

A comparison between the measured heat transfer rate at the front stagnation point and the heat transfer rate in the same region from Lowery and Vachon [3] is given in Table 1. It can be seen that the measured values exceed those of Lowery and Vachon [3] by some 12%, with the exception of the 25 m/s test which is higher by around 25%. The reason for this is not clear. From Zukauskas and Ziugda [9], transition of the boundary layer is expected to commence when the product of upstream turbulence intensity times Reynolds number ($Tu\ Re$) is greater than 1500. Thus, the fact that transition to turbulence commences at a

Table 1. Comparison of surface heat flux in the front stagnation region

U [m/s]	Re	Tu [%]	$Tu\ Re$	$Tu\ Re^{0.5}$	$Nu_{fsp}/Re^{0.5}$ Measured	Lowery and Vachon [3]
5	7190	8.5	611.2	7.2	1.35	1.20
10	14 380	7.9	1136.0	9.5	1.38	1.24
15	21 580	7.4	1596.9	10.9	1.44	1.27
20	28 760	7.2	2070.7	12.2	1.47	1.30
25	35 950	6.9	2480.6	13.1	1.66	1.32
30	43 140	6.8	2933.5	14.1	1.53	1.35

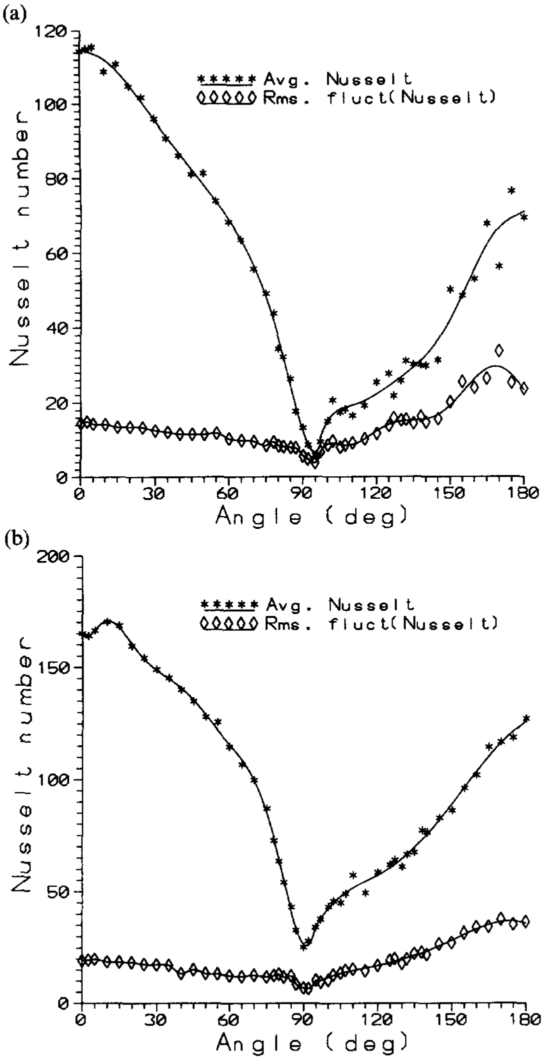

Fig. 1. Variation in local Nusselt number: (a) Re = 7190, (b) Re = 14380.

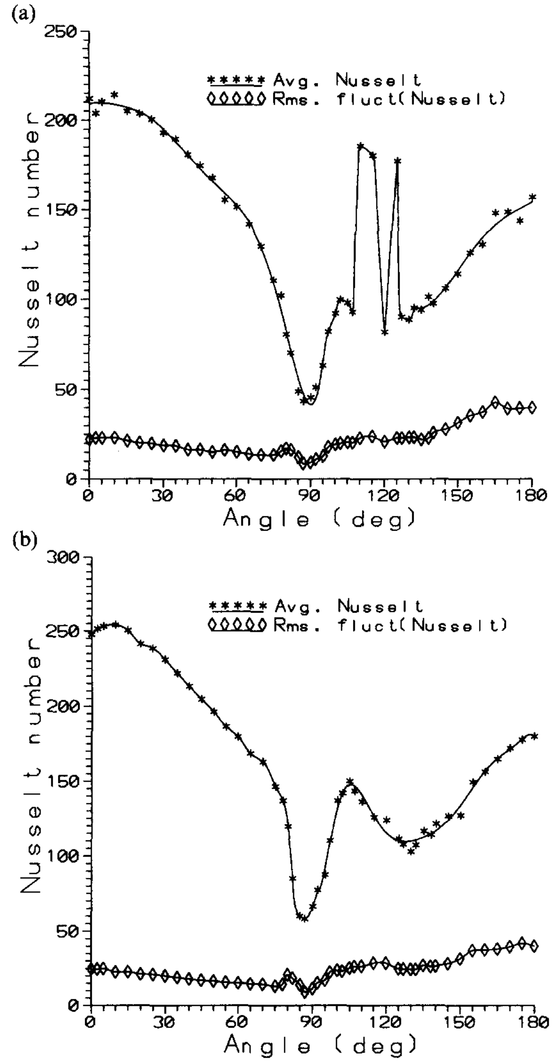

Fig. 2. Variation in local Nusselt number: (a) Re = 21 580, (b) Re = 28 760.

Reynolds number of around 21 000, as suggested by Fig. 2(a), is supported by the value of 1597 for $Tu\,Re$ from Table 1.

The difference in heat transfer character between a case in which the boundary layer remains laminar until separation and one in which the boundary layer becomes turbulent is illustrated by Fig. 4 which shows the plots for a Reynolds number of 43,140 for both low and high turbulence cases. It can be seen that the Nusselt number pattern for the laminar case exhibits the characteristic features of a minimum Nusselt number at the separation angle (80°), followed by an increase in heat transfer in the wake region. At the higher turbulence level, the first minimum at 90° represents boundary layer transition, whereas the second minimum relates to separation of the turbulent boundary layer. From the rms plots, it is evident that the heat transfer fluctuations over the front of the tube are much higher for the mainstream turbulence level of 6.8%. For the back of the tube it can be seen that the fluctuations in heat flux are higher for the high flow turbulence case in the region where the turbulent boundary layer is still attached to the surface. Once both boundary layers have separated, however, the level of fluctuation in the heat transfer rate is higher for the low turbulence case. This is a consequence of more mixing of fluid in this area due to the wider wake associated with early separation of the laminar boundary layer.

The circumferentially averaged Nusselt number and the average level of Nusselt number fluctuations for the range of Reynolds numbers are summarised in Table 2. Comparison with the equivalent data for the low turbulence tests from Part I (Table 3) indicates that the average level of the Nusselt number fluctuations has increased. This is a consequence of the large increase in fluctuations over the front of the cylinder, although for tests with boundary layer tran-

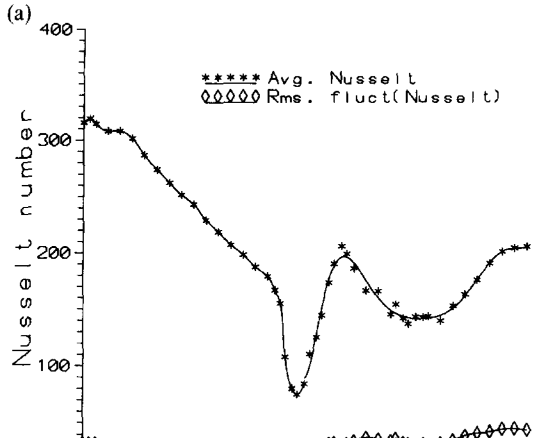

Fig. 3. Variation in local Nusselt number: (a) Re = 35 950, (b) Re = 43 140.

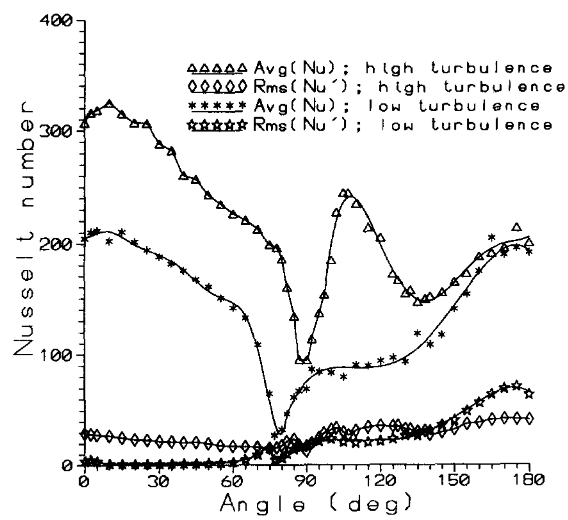

Fig. 4. Effect of freestream turbulence on Nusselt number variation, Re = 43 140.

Table 2. Nusselt number fluctuations for highly turbulent flow

Re	avg (Nu)	avg (rms(Nu'))	avg (rms(Nu')) [%]
7190	56.9	13.9	24.5
14 380	100.0	18.9	18.9
21 580	139.5	22.3	16.0
28 760	163.5	23.9	14.6
35 950	198.9	28.5	14.3
43 140	216.5	27.7	12.8

sition this is partly compensated by the lower level of fluctuations at the back. Because the average Nusselt number has also increased, the Nusselt number fluctuations expressed as a percentage have not changed significantly. Although no exactly comparable measurements are reported in the literature, The Nusselt number fluctuations summarised in Table 2 are in the same range as the 18–20% unsteadiness in stagnation region heat transfer recorded by Ching and O'Brien [5] for a freestream turbulence of 8% and Reynolds numbers of 136 000 to 170 000.

Time traces of unsteady heat flux

Figure 5 shows the time variation of the heat flux at the Reynolds number of 43 140 for a sample period of 0.15 s. Results are presented for three cases: 0° and 15° without the turbulence grid and 15° with the grid. For the front stagnation point with no grid, a clear periodicity corresponding to twice the vortex shedding frequency is apparent. At 15° with no turbulence grid, the heat transfer fluctuations are low in magnitude but a distinct periodicity corresponding to vortex shedding can be detected. When the turbulence level of the mainstream is increased to 6.8%, there is no evidence of periodicity and the magnitude of the heat transfer fluctuations increases by a factor of 25.

Heat transfer auto spectra

Figure 6 shows the heat transfer auto spectra for a number of angular positions at the Reynolds number of 43 140. In Figs. 6(a) and (b), the spectra for the low turbulence conditions are presented, and the results are similar to those reported for the Reynolds number of 21,580 as described in Part I. At 0°, the largest peak at 520 Hz corresponds to the double vortex shedding frequency although the single shedding frequency (260 Hz) and a number of harmonics are also evident. At 15° only the vortex shedding frequency can be seen whereas at 80°, which corresponds to separation, the double frequency is again evident. In Fig. 6(b), for positions following separation, it can be seen that the auto spectra levels are much higher, corresponding to the higher rms level of the heat transfer fluctuations in this region. It can also be seen that there is no evidence of the vortex shedding frequency,

Table 3. Comparison of measured vortex shedding frequencies

	Low turbulence level		High turbulence level	
Reynolds no.	Frequency [Hz]	Strouhal number	Frequency [Hz]	Strouhal number
7190	42	0.210	42	0.210
14380	86	0.215	88	0.220
21580	128	0.213	136	0.227
28760	172	0.215	188	0.235
35950	216	0.216	244	0.244
43140	256	0.213	300	0.250
50350	300	0.214	—	—

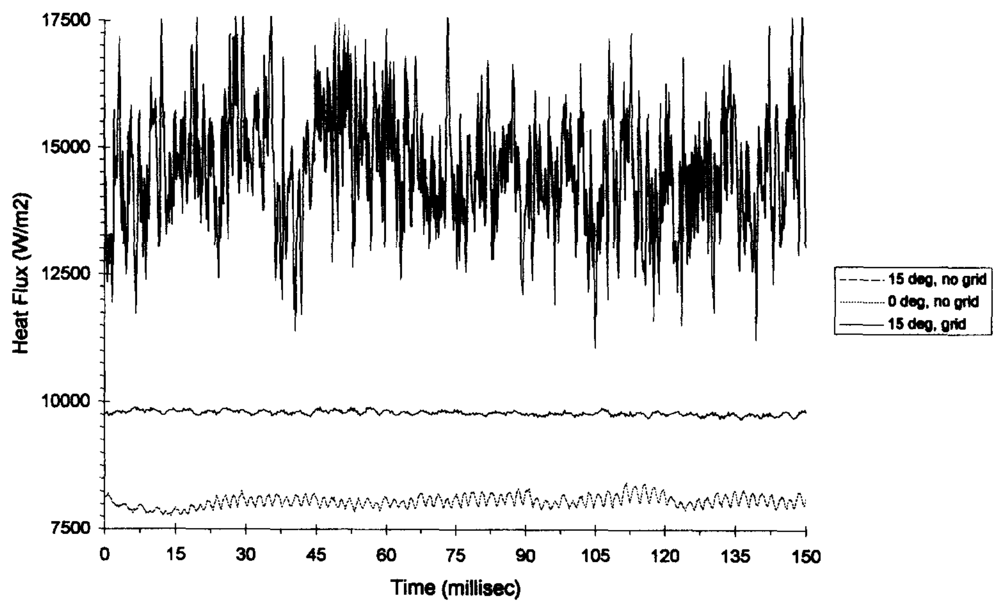

Fig. 5. Heat flux time traces at two turbulence levels, $Re = 43\,140$

with the exception of a small peak for the 155° location.

In Fig. 6(c), for the front of the cylinder with high freestream turbulence levels, it is clear that there is no evidence of periodicity and that the level of high frequency fluctuations is substantially higher than for the low turbulence case. It can also be seen that the level of fluctuations decreases with increasing distance from the front stagnation point. This is in keeping with the rms level of the Nusselt number fluctuations shown in Fig. 3. Over the rear of the cylinder, comparison of Fig. 6(d) with Fig. 6(b) indicates similar trends for the two turbulence levels. The small vortex shedding peak detectable for the 155° location is also visible for the high turbulence case, but the frequency of vortex shedding has shifted to a higher frequency (300 Hz). The higher shedding frequency for this case can be explained by the wake narrowing associated with the later separation of the turbulent boundary layer as compared with the laminar layer, when considered in the context of the von Karman stability criterion for vortex streets, Lamb [10]. A comparison between vortex shedding frequencies for the low turbulence and high turbulence cases is given in Table 3. It can be seen from this table that the shedding frequency stay approximately equal for the lower velocities, where the combination of velocity and turbulence level is not enough to trigger transition of the boundary layer. The Strouhal number obtained for these cases is the classic value of approximately 0.21. For the cases in which the high mainstream turbulence level coupled with the increasing velocity trigger transition of the boundary layer, however, the Strouhal number exceeds this standard value.

Simultaneous velocity and heat transfer data

Figure 7 shows the auto spectra of velocity and heat flux, measured at 65°, for a test conducted with a Reynolds number of 21,580 and a turbulence intensity of 7.4%. The 65° location was chosen as representative

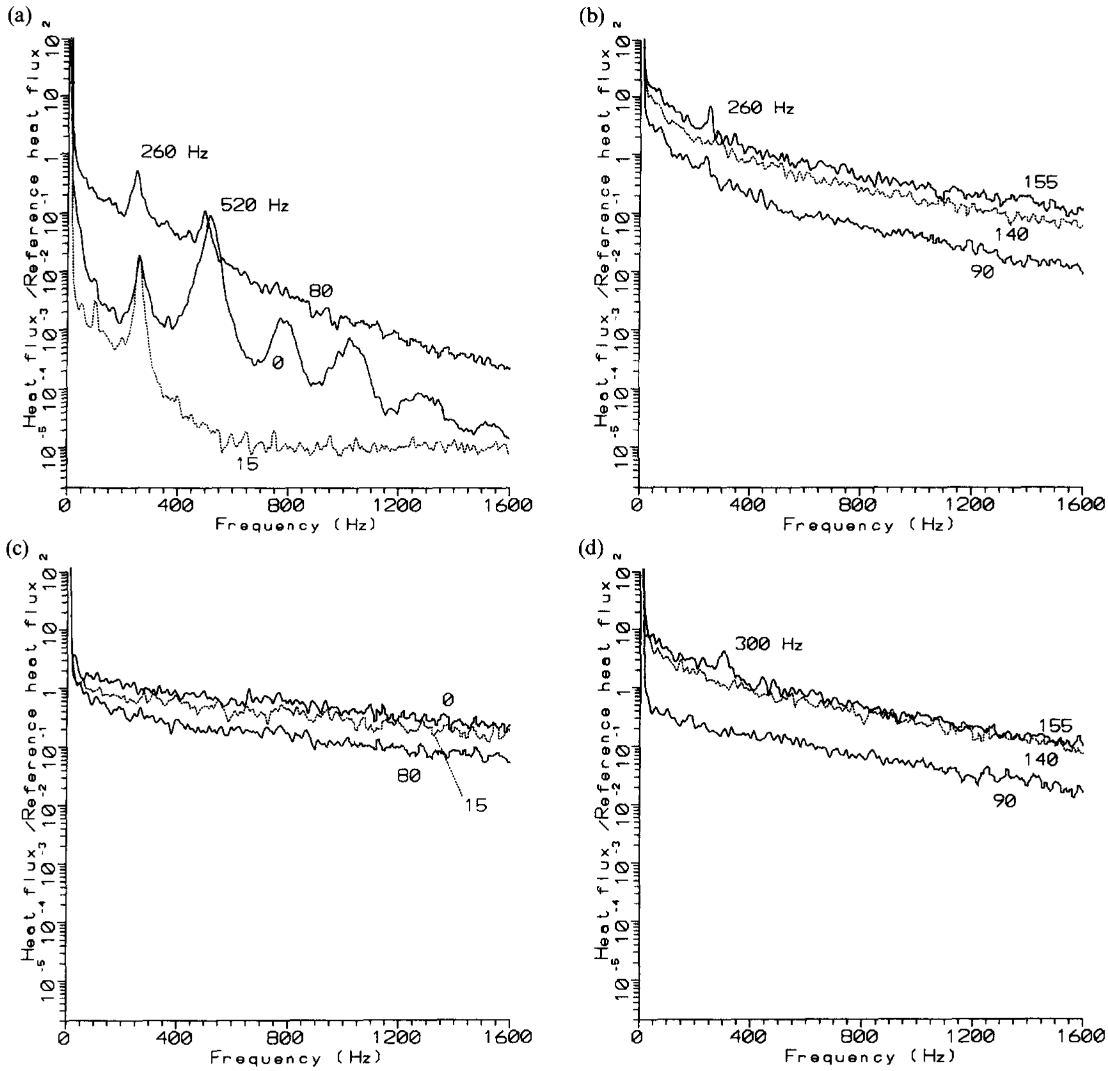

Fig. 6. Heat transfer auto spectra at two turbulence levels: (a) low Tu, front of cylinder; (b) low Tu, back of cylinder; (c) high Tu, front of cylinder; (d) high Tu, back of cylinder.

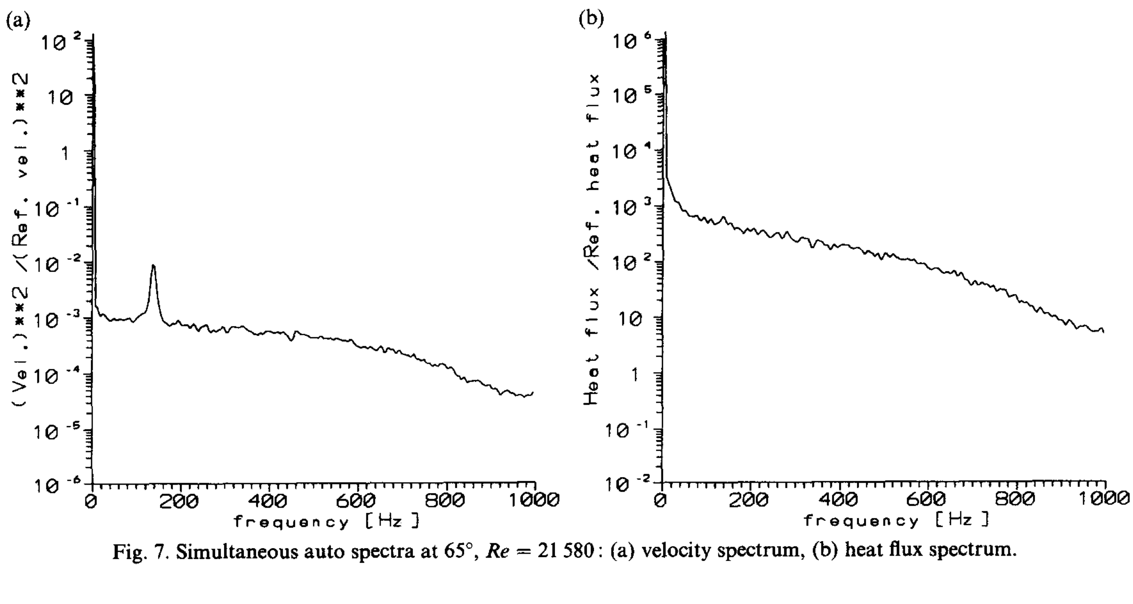

Fig. 7. Simultaneous auto spectra at 65°, $Re = 21\,580$: (a) velocity spectrum, (b) heat flux spectrum.

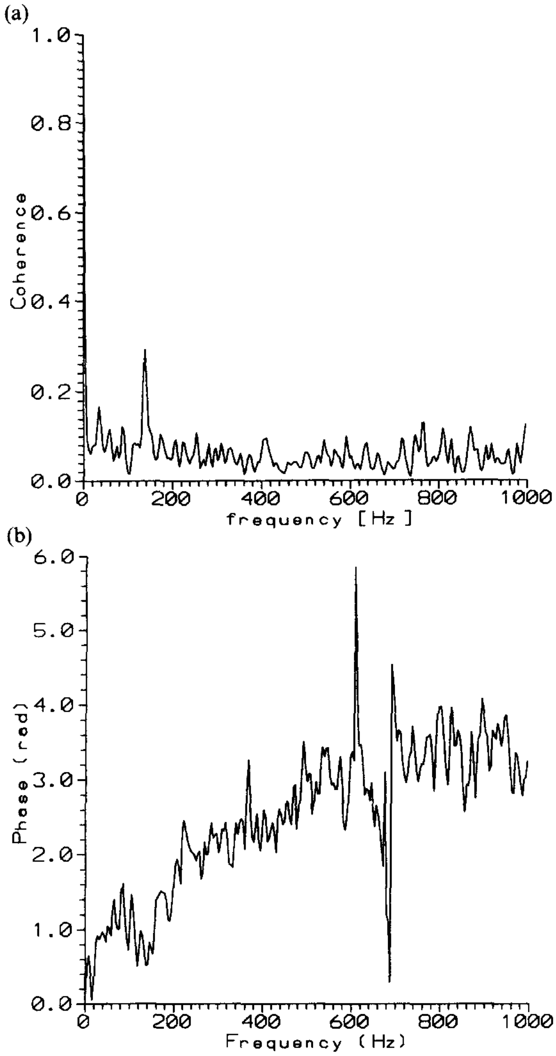

Fig. 8. Coherence between velocity and heat flux, $Re = 21\,580$.

of locations preceding boundary layer separation and was used also for the low turbulence tests of Part I. The velocity measurements were made at a distance of 1 mm from the surface measurement point, in a radial direction. From Fig. 7(a) it can be seen that although the general level of velocity fluctuations has increased, as compared to the low turbulence case of Part I, there is still a strong peak at the vortex shedding frequency. In contrast, for the heat transfer data, Fig. 7(b) shows that the rise in the general level of heat transfer fluctuations is so significant that the peak associated with vortex shedding cannot be detected. Despite this, a peak in coherence at the vortex shedding frequency, shown in Fig. 8(a), indicates that the surface heat flux is influenced to some degree by velocity fluctuations linked to vortex shedding. However, the low level of coherence indicates that only a small part of the heat transfer fluctuations originates in vortex shedding. The remainder of the fluctuations are considered to originate in the turbulent eddies present in the highly turbulent flow, as discussed in the following section.

DISCUSSION

Unlike the phase plot for the simultaneous measurements in the low turbulence case (Part I), Fig. 8(b) shows that there is a very distinct phase difference between the fluctuations in surface heat flux and the fluctuations in velocity measured 1 mm away from the surface. For the low turbulence case, the fluctuations in velocity outside the wake region were shown to originate in pulsation of the entire flow field as a consequence of vortex formation and shedding. In contrast, for the high turbulence case, most of the velocity fluctuations are due to the transport of small turbulent eddies within the main flow. The radial motion of these eddies will have a significant influence on surface heat flux, but the low radial velocity results in a time delay between the measured velocity and heat transfer fluctuations. This shows up in the steep slope of the phase difference for the high turbulence case. The dip in the phase plot around the vortex shedding frequency is a consequence of part of the fluctuations originating in vortex formation and shedding with an associated zero phase difference. Furthermore, beyond a frequency of around 600 Hz, the phase difference flattens out as a consequence of the zero phase difference from the higher content of step noise in this frequency range, Scholten [11].

To verify the suggested link between radial eddy velocity and the measured phase difference between surface heat transfer fluctuations and velocity fluctuations 1 mm above the surface, an order of magnitude analysis can be performed. From the phase difference shown in Fig. 8(b), a phase shift of π is estimated for a frequency of 500 Hz. Using the relation between phase difference and frequency to calculate the corresponding time delay results in:

$$\Delta t = \frac{\text{phase}}{2\pi\text{freq}} = 0.001\ \text{s}, \tag{1}$$

i.e. a time delay of approximately 1 msec exists between the fluctuations in measured heat transfer and velocity. The time delay can also be estimated from consideration of the local velocity together with the distance of 1 mm between the two measurement locations. The local velocity, measured by the LDA, has an average value of 22.7 m/s and a turbulence intensity of 4.75%, giving an rms value of 1.08 m/s for the velocity fluctuations. When these fluctuations are viewed as originating in the existence of small turbulent eddies, the velocity fluctuations in the radial direction (perpendicular to the cylinder surface) can be taken to be equal in magnitude to the measured tangential velocity fluctuations. This means that the measured rms value can be viewed as the average velocity with which small vortices are transported in the radial direction. Together with the 1 mm distance of the laser measurement volume from the cylinder surface, this leads to a time delay from the radial eddy velocity of:

$$\Delta t = \frac{\text{distance}}{\text{velocity}} = 0.0009\,\text{s}, \qquad (2)$$

which is of the same order of magnitude as the 1 msec time delay calculated from the phase plot of Fig. 8(b). It can therefore be concluded that the measured phase difference between the fluctuations in velocity and the fluctuations in surface heat flux is indicative of the radial transport of small turbulent eddies as the origin of the measured heat transfer fluctuations. Although this analysis is based on a single set of data, simultaneous measurements obtained in a small array of cylinders appear to support the finding that, for highly turbulent flows, the surface heat flux is strongly influenced by the radial motion of eddies, Scholten [11].

CONCLUSIONS

A system has been developed to measure rapidly fluctuating heat transfer from cylinders in cross flow, by means of a fast response hot film sensor. In conjunction with this, a single component laser Doppler system has been used to simultaneously measure the time-resolved local velocity. From the results obtained for a cylinder in cross flow with a high level of freestream turbulence, the following conclusions can be drawn:

1. The level of fluctuations at the front of the cylinder is increased dramatically as compared to the level of fluctuations reported in Part I for cylinders in a low turbulence cross flow. This time variation of the heat flux at the front of the cylinder has, in contrast to the low turbulence case, no evidence of any periodicity but is highly random in character. For the back of the cylinder, the magnitude of the heat transfer fluctuations is approximately equal to the magnitude of fluctuations recorded for the low turbulence cases. An exception to this exists for those tests in which the combination of flow Reynolds number and freestream turbulence level is sufficient to trigger transition to turbulence of the attached boundary layer. In these cases, the level of heat transfer fluctuations for the high turbulence tests is higher in the region where the turbulent boundary layer exists, but lower in the wake region at the very back of the cylinder. This local region of low heat transfer fluctuations is a consequence of less mixing of the fluid within the wake region due to the narrower wake associated with delayed separation of the boundary layer.
2. When the auto spectra of the local heat flux around the circumference of the cylinder are examined, it can be seen that limited evidence of periodicity at the vortex shedding frequency can be found in the wake region only. This small evidence of vorticity shows that the frequency of vortex shedding is increased, as compared to the low turbulence cases of Part I, for those cases in which the boundary layer has become turbulent. This is in keeping with the wake narrowing that occurs for these test conditions.
3. From simultaneous velocity and surface heat flux measurements it can be concluded that only a small part of the heat transfer fluctuations at the front of the cylinder are linked to vortex formation and shedding at the back of the cylinder, with the remainder of the heat transfer fluctuations originating in the small turbulent eddies present in the highly turbulent flow. The phase difference determined from these simultaneous measurements is shown to be indicative of the low velocity perpendicular to the cylinder surface that governs the radial movement of turbulent eddies.

Acknowledgement—The authors appreciate the assistance of Prof. J. A. Fitzpatrick with the spectral analysis procedures.

REFERENCES

1. Morgan, V. T., The overall convective heat transfer from smooth circular cylinders. *Advances in Heat Transfer*, 1975, **11**, 199–264.
2. Dyban, E. and Epick, E., Some heat transfer features in the air flow of intensified turbulence, *Proc. 4th Int. Conf. on Heat Transfer*, Paris, Vol. 2, 1970, Paper FC 5.7.
3. Lowery, G. W. and Vachon, R. I., The effect of turbulence on heat transfer from heated cylinders, *Int. J. Heat Mass Transfer*, 1975, **18**, 1229–1242.
4. Simmons, S. G., Hager, J. M. and Diller, T. E., Simultaneous measurements of time-resolved surface heat flux and freestream turbulence at a stagnation point, *Proc. 9th Int. Heat Transfer Conf.*, Vol. 2, Hemisphere, Washington, DC, 1990, pp. 375–380.
5. Ching, C. Y. and O'Brien, J. E., Unsteady heat flux in a cylinder stagnation region with high freestream turbulence, *Fund. Exp. Meas. in Heat Transfer*, ASME HTD 179, 1991, pp. 57–66.
6. Beasley, D. E. and Figliola, R. S., A generalised analysis of a local heat flux probe, *J. Phys. E.: Sci. Instrum.*, 1988, **21**, 316–322.
7. Simon, L., Scholten, J. W. and Fitzpatrick, J. A., Velocimetrie laser: amelioration du traitement des donnees experimentales par interpolation d'ordre 1. *Proc. Congres Francais de Mechanique*, Strasbourg, 1995, pp. 321–324.
8. Scholten, J. W. and Murray, D. B., Measurement of convective heat transfer using hot film sensors: correction for sensor overheat, *J. Heat Transfer* Trans. ASME, 1996, **118**(4), 982–984.
9. Zukauskas, A. and Ziugda, J. *Heat Transfer of a Cylinder in Cross Flow*, ed. G. F. Hewitt, Hemisphere Publishing Corporation, 1985.
10. Lamb, H., *Hydrodynamics*, 6th edn, University Press, Cambridge, 1932.
11. Scholten, J. W., Fluctuating heat transfer of cylinders in cross flow, Ph.D. thesis, University of Dublin, Trinity College, Dublin, 1996.